Effects of Atmospheric Turbulence on a Quadrotor Heavy Lift Airship

Mark B. Tischler*
U.S. Army Research and Technology Laboratories, Moffett Field, California
and
Henry R. Jex†
Systems Technology, Inc., Hawthorne, California

The response of a quadrotor heavy lift airship (HLA) to atmospheric turbulence is evaluated using a four-point input model. Results show interaction between gust inputs and the characteristic modes of the vehicle's response. Example loop closures demonstrate tradeoffs between response regulation and structural loads. Vehicle responses to a tuned discrete wavefront compare favorably with the linear results and illustrate characteristic HLA motion.

Nomenclature

a_z = acceleration of the hull center of gravity along the positive (downward) z-body axis, ft/s^2 (g)
C_w = traveling upgust wave celerity, i.e., inertially referenced crest velocity, ft/s
dB = decibels, = 20 $\log_{10}$ (gain)
$F_{c_{zl}}$ = constraint force exerted on the hull support structure at the attachment point of LPU-1, along the positive (downward) z-body axis, lb
LPU = lift propulsion unit, each comprised of one rotor, one propeller, and one nacelle; numbering system shown in Fig. 2.
L_{w_g} = characteristic scale length for vertical turbulence, ft
ℓ_h = hull length, ft
s = Laplace transform operator
T_h, T_h' = heave mode time constants for the open-loop (bare airframe) and closed-loop (control system engaged) vehicle, respectively,s (time-to-half-amplitude = 0.693 T; $T = T_h, T_h'$)
V_a = reference relative airspeed, ft/s
V_0 = reference inertial velocity along the x-body axis (ground speed), ft/s
w = velocity of the hull center of gravity along the positive (downward) z-body axis, ft/s
w_c = heave axis control deflection, $w_c = 1$ deg $\rightarrow$ 1 deg of negative collective pitch on each rotor, deg
$w_g^{s1}, w_g^{s2}, w_g^{s3}, w_g^{s4}$ = gust velocities along the inertial z axis at input sources 1-4, respectively; positive downward, ft/s
θ, ϕ = pitch and roll Euler angles, respectively, rad (deg)
σ = root-mean-squared (rms) value
σa_z = root-mean-squared(rms) level of hull acceleration, a_z
$\sigma F_{c_{zl}}$ = root-mean-squared(rms) level of vertical constraint force at LPU-1 ($F_{c_{zl}}$)
σ_{w_g} = intensity level (rms) for turbulence along the inertial z axis, ft/s
$\Phi_{w_g w_g}, \Phi^*_{w_g w_g}$ = power spectral desity function and truncated power spectral density function, respectively, for vertical turbulence, ft^2/rad-s
ω = frequency, rad/s
ω_{BW_h} = heave control system bandwidth; defined as the -3 dB frequency (Fig. 3), rad/s
ω_c = Butterworth filter cutoff frequency, rad/s
ω_p, ω_p' = pitch oscillation mode frequencies for the open-loop (bare airframe) and closed-loop (control system engaged) vehicle, respectively, rad/s
ψ_w = traveling upgust wave encounter angle (Fig. 2), deg

Superscripts

$\bar{(\ )}$ = average value
$\dot{(\ )}$ = time derivative with respect to nonrotating axes

Introduction

THE effects of atmospheric turbulence on the airship motions and structures are a continuing concern.[1-3] Low-speed and mooring operations are especially difficult, since the reduced control power and ground clearance increase the vehicle's vulnerability to turbulence. Recently, the British AD-500, Goodyear Columbia, and Aerolift Cyclocrane have suffered considerable damage in mooring accidents, which are largely attributable to severe turbulence.

Current design concepts emphasize requirements of precision vehicle control and gust response suppression in low-speed and hover-flight operations.[4,5] These requirements are especially formidable for the heavy lift airship (HLA) logging configuration[6] and the Maritime Patrol Airship (MPA).[4] The utility of these vehicles depends on their ability to operate in all weather conditions.

Presented as Paper 82-1542 at the AIAA Ninth Atmospheric Mechanics Conference, San Diego, Calif., Aug. 9-11, 1982; submitted Aug. 12, 1982; revision received April 11, 1983.

*Research Scientist, Aeromechanics Lab., Ames Research Center; formerly, Staff Engineer, Research, Systems Technology, Inc., Hawthorne, Calif. Member AIAA.

†Principal Research Engineer. Associate Fellow AIAA.

Studies by DeLaurier[1] on the effects of atmospheric turbulence on conventional airships showed the existence of significant coupling between airship pitch dynamics and vehicle structural loads. Maximum vehicle response and attendant loads were found to occur for turbulence wavelengths that correspond to those of the airships' normal modes. Nagabhushan[2] analyzed the effects of closed-loop control on the hovering performance of quadrotor HLAs in crosswind flight conditions. His analysis showed that considerable improvement in the radius of hover could be achieved by feedbacks of inertial vehicle position to the rotor cyclic controls. The associated effects on the structural loads of HLAs were not investigated.

An analysis of the dynamics and performance of a generic quadrotor heavy lift airship (Fig. 1) using the joint Systems Technology, Inc. (STI) and National Aeronautics and Space Administration (NASA) simulation was discussed in Refs. 7 and 8. One significant conclusion was that gust accelerations have a considerable impact on the loads experienced by airships due to apparent mass effects. This will be especially important for the HLA logging mission, where large and rapid changes in the local atmospheric conditions result from the geographic surroundings.

In this paper, we further develop analysis of turbulence effects on quadrotor heavy lift configurations with the use of the four-point atmospheric input model outlined in Refs. 7 and 8. This multiple-input model allows a more accurate description of gust-gradient effects than is obtainable with a more conventional single-point aircraft model.[9] An assessment of the effects of atmospheric turbulence on the vehicle dynamics was made with an adaption of design military gust specifications for piloted aircraft[10] (MIL-F-8785C). This paper presents an overview of the four-point atmospheric input model, a discussion of its range of validity, and an application of the military specification for a typical low-speed unloaded flight condition. The results show the effects of closed-loop control on vehicle turbulence response and associated structural loads.

Atmospheric Input Model

Analyses of turbulence effects on aircraft are generally based upon the assumption that the local atmosphere may be represented by gust velocities and linear gradients at a single point (nominally the aircraft center of gravity), then extrapolated outward therefrom. As noted by Etkin,[9] this leads to significant overestimation errors for large aircraft and small gust wavelengths. Airships, with their nearly neutral buoyancy, large dimensions, and relatively low cruise speeds, are especially sensitive to large-scale atmospheric gradients and accelerations. A multiple-point input model allows the calculation of these gradient effects at smaller wavelengths (and larger aircraft size) than is possible with a single-point model. This results from the spatial interpolation scheme, which is used to calculate average gradients and velocities from the velocities at the various input sources. Based upon these considerations, we have implemented a four-point atmospheric input model, which is an extension of the work of Holley and Bryson[11] and Etkin,[9] and is discussed in detail in Refs. 7 and 8.

Figure 2 shows the locations of the four input sources for the present analysis, which are selected as a compromise to be closed to the more distal vehicle components [i.e., hull ends, tail surfaces, and lift/propulsion units (LPUs)]. These sources are assumed to be statistically uncorrelated because of their large separation relative to gust characteristic lengths at low altitudes. Hence, linear superposition can be used to determine the total (Gaussian) turbulence response of the vehicle by summing the isolated responses of the vehicle to individual gust velocity sources. Each input gives rise to effective gust accelerations, velocities, and gradients at the hull, tail, and LPUs. These, in turn, are used to calculate aerodynamic forces and moments for use in the dynamic equations of motion. The many interpolation formulas and equations for the associated aerodynamic forces are presented in Ref. 7 and are not repeated here.

Discrete wave fronts are generated by tailored sequencing among the input sources. These waves can be tuned to the vehicle's dynamic modes to evaluate critical non-Gaussian phenomena. The four-point model is valid for all discrete disturbances within the assumption of linear interpolation of local gust velocity between input sources.

The use of a four-point atmospheric model allows the calculation of gradient effects to shorter gust wavelengths than is possible with a single-point model; however, a lower gust wavelength limit exists on the validity of the model in simulating the response to sinusoidal inputs. This results from the assumption of gust velocity linear interpolation between the various input sources and the use of a closed-form hull aerodynamic model dependent only on the relative motion between the hull center of volume and air mass.

Analyses using a multiple-segment hull model[1] show that the response power spectra fall off rapidly for gust wavelengths shorter than twice the hull length ($2\ell_h$). This is due to the pressure averaging effect of the hull. In the present analysis, the spectral-power reduction is modeled with a third-order Butterworth filter. The filter break frequency corresponds to a wavelength of $2\ell_h$, the assumed limit of the four-point input model.

While the more accurate multiple-segment model is necessary to evaluate distributed structural loads along the airship hull, the simplified approach adopted here is felt to be sufficient for dynamics and control analyses of heavy lift airships, where the loads between widely separated elements are of prime inportance. This approach allows the easy incorporation of measured atmospheric data (e.g., at four towers more than 100 ft apart) and is well suited for the study of vehicle responses to discrete waveforms, such as traveling gust "waves" and thermal currents. A comprehensive ex-

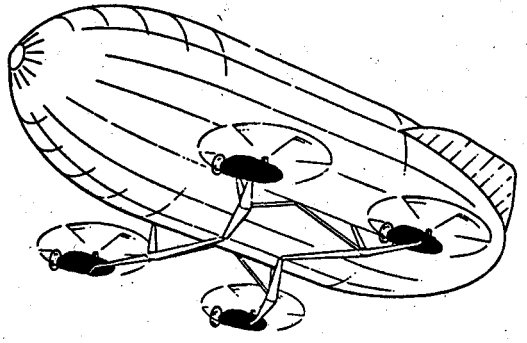

Hull	
Length	240 ft
Diameter	103 ft
Volume	1.5×10^6 ft^3
Tail area	2520 ft^2
Weight	8.89×10^4 lb
Lift propulsion unit (LPU)	
Rotor diameter	56 ft
Propeller diameter	13 ft
Engine horsepower (One per LPU)	1524 hp
Weight (each LPU)	9×10^3 lb

Composite vehicle	Unloaded	Loaded
Weight (lb)	125,000	165,000
Buoyancy ratio	0.92	0.70

Fig. 1 Generic quadrotor heavy lift airship used in present study.

perimental effort with an instrumented flight vehicle would be needed to validate the preceding assumptions.

Analysis Techniques

The present analysis procedures are broadly based on the MIL-F-8785C turbulence requirements.[10] This specification requires analysis of both continuous random (Gaussian) statistical turbulence and discrete (non-Gaussian) disturbances. As noted by Etkin,[9] statistical analyses account for the Gaussian loads up to 3σ, important for fatigue assessment. The discrete turbulence (wave front) analysis accounts for the critical loads which occur in thunderstorms with far greater frequency than their Guassian probability (*Pr* $4.5\sigma = 7 \times 10^{-6}$) would indicate. A discussion of the application of these analysis techniques to the four-point atmospheric model is presented below.

Statistical Turbulence Analysis

The longitudinal gust response transfer functions for each input source (e.g., θ/w_g^{s1}, a_z/w_g^{s2}, *etc.*) are generated by exercising the numerical linearization option of the STI/NASA heavy lift airship simulation.[7] These transfer functions provide valuable insight into the dynamics of HLA gust responses. Constraint force transfer functions give the gust-imparted loads in the support structure between the central buoyant envelope (hull) and the LPUs. Statistical information is obtained through analysis of the gust transfer functions and the relevant atmospheric spectra. In the present analysis we used a simplified form of the Dryden model[12] with the high-frequency spectrum truncated for wavelengths shorter than twice the hull length ($2\ell_h = 480$ ft). The turbulence model's scale length and intensity parameters were obtained from Ref. 10. Open-loop (bare airframe) and closed-loop (flight control system engaged) studies were completed to investigate tradeoffs between requirements for response suppression and structural integrity.

Discrete Gust Response

Discrete gust responses show the vehicle reaction to non-Gaussian disturbances. A tuned upgust wave front was developed based on the Military specification guidelines.[10] This wave consists of sequenced $(1-\cos\omega t)$ discrete waves, one at each of the four input source locations, designed to excite the vehicle at its natural frequencies of motion about the pitch and roll axes. The resulting large-amplitude time histories provide information on critical loads and motions.

Linearized Transfer Functions

The open-loop linearized and decoupled longitudinal transfer functions were calculated for a flight condition of 44 ft/s (13.4 m/s) (axial airspeed), which corresponds to that analyzed in Ref. 8. The present model includes the effect of aerodynamic interference among the vehicle components (e.g., hull/rotor, rotor/tail, etc.). A comparison of the present transfer functions with those of Ref. 8 shows interference effects on the vehicle's transient dynamics to be small to negligible. As noted in Ref. 7, the dominant effects are changes to vehicle trim controls and power conditions.

Closed-loop transfer functions were calculated for the nominal flight control system described in Ref. 8. Feedbacks of attitude and *inertial* linear and angular velocities to the rotor, propeller, and tail control surfaces stabilize the vehicle against unwanted motion and maintain the commanded flight path. A forward loop integrator is used in each axis to insure zero steady-state error.

Figure 3 shows the vertical velocity response (w) to vertical command inputs (w_c) for the open-loop (feedbacks disconnected) and closed-loop (feedbacks connected) vehicle. The

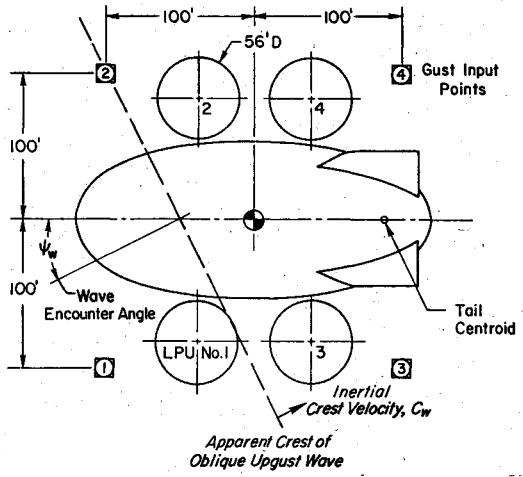

Fig. 2 Atmospheric input model.

open-loop response is characterized by the dominant heave mode frequency ($1/T_h = 0.22$ rad/s), the pitch oscillation mode frequency ($\omega_p = 0.27$ rad/s), and the -3 dB heave bandwidth ($\omega_{BW_h} = 0.36$ rad/s). When the nominal feedback gains are used, the pitch oscillation mode is well damped, and the augmented heave mode frequency is increased ($1/T_h' = 0.85$ rad/s). The associated increased heave bandwith ($\omega_{BW_h} = 0.8$ rad/s) implies improved command following and disturbance suppression characteristics. Attendant effects on gust-induced structural loads was a central question of the present study and is discussed in the following sections.

Additional increases in the vertical velocity feedback gain results in higher bandwidth systems (Fig. 3) with further improvements in the dynamic characteristics. Increased gains result in larger control deflections, which may cause surface limiting in heavily loaded conditions. However, for the present unloaded flight condition, this is not a problem, even for very high bandwidth systems ($\omega_{BW_h} = 5$ rad/s).

The gust transfer functions examined in the study were: pitch attitude, θ; vertical acceleration at the hull center of gravity, a_z; and vertical constraint force exerted on the hull structure at the attachment point of LPU-1, $F_{c_{z1}}$. These variables exemplify the motions and loads which are characteristic of the vehicle longitudinal response to turbulence.

Pitch Attitude Response

The open- and (nominal) closed-loop pitch attitude responses to vertical gusts on input source 1, θ/w_g^{s1}, are shown in Fig. 4. The vehicle pitch response to input source 1 is representative of the response of the vehicle to the other gust input sources ($w_g^{s2}, w_g^{s3}, w_g^{s4}$). This results from the assumed symmetrical distribution of the gust input sources about the hull center of volume, the hull's fore/aft symmetry, and the relatively small tail compared to the hull. The transfer functions for gust inputs sources 3 and 4 have a slightly higher gain in the high-frequency region. This is due to the unsteady tail forces, which are predominantly influenced by the rearward sources ($s3$,$s4$).

Referring to Fig. 4, we note that the open-loop dominant pitch response is at the damped natural pitch oscillation frequency ($\doteq \omega_p$) as expected. These results agree with those of DeLaurier,[1] who also showed maximum gust responses at vehicle damped pitch natural frequencies. The peak closed-loop response is significantly reduced from the open-loop case due to the desired function of the pitch attitude control system. In the frequency range above, the nominal closed-loop bandwidth($\doteq$highest closed-loop pole, $1/T_h'$), the open- and closed-loop transfer functions are identical; therefore, the initial time responses (i.e., slopes) for both cases will also

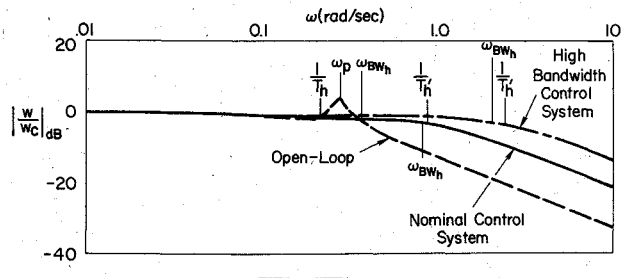

Fig. 3 Vertical velocity response to heave command inputs.

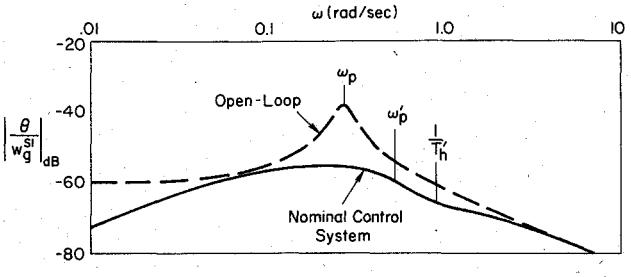

Fig. 4 Pitch attitude response to gust inputs at source 1, θ/w_g^{s1}.

match. For low-frequency inputs, the attitude response asymptotically approaches zero due to the installed trim integrator. These linear results correlate well with nonlinear time histories of Ref. 8 and those presented in the next section.

Vertical Acceleration Response

As with the pitch response, the vertical acceleration (a_z) transfer functions are quite similar among the four input sources. This again is due to the symmetrical orientation of the sources about the hull center of volume and the small relative size of the tail. The acceleration response to a vertical gust on input source 1 (a_z/w_g^{s1}) is shown in Fig. 5 for the open- and closed-loop systems.

Ignoring the excitation of the pitch oscillation mode (ω_p), we obtain from Fig. 5, the following approximate relationship between the vehicle open-loop vertical acceleration response and the gust acceleration at input source l:

$$a_z \doteq s\left(\frac{w_g^{s1}}{4}\right) = \frac{\dot{w}_g^{s1}}{4} \tag{1}$$

The approximately identical results of the remaining input sources give:

$$a_z \doteq \bar{\dot{w}}_g \tag{2}$$

where

$$\bar{\dot{w}}_g = \frac{(\dot{w}_g^{s1} + \dot{w}_g^{s2} + \dot{w}_g^{s3} + \dot{w}_g^{s4})}{4} \tag{3}$$

Equation (2) indicates that the open-loop vehicle is subject to pure convective motion. This results from the near-neutral buoyancy ratio condition (0.92) of the present vehicle. Analyses by DeLaurier[1] and Nagabhushan[2] verify this conclusion for other neutrally buoyant vehicles. Conceptually the open-loop vehicle may be considered as a soap bubble or particle in the air mass, convecting with the local motion.

This result is especially important for mooring and other power-off flight conditions; attempts to restrain the vehicle will require the attachment structures between the hull and LPU to absorb the large energy of the local air mass motions. This explains the historical policy of allowing airships to float

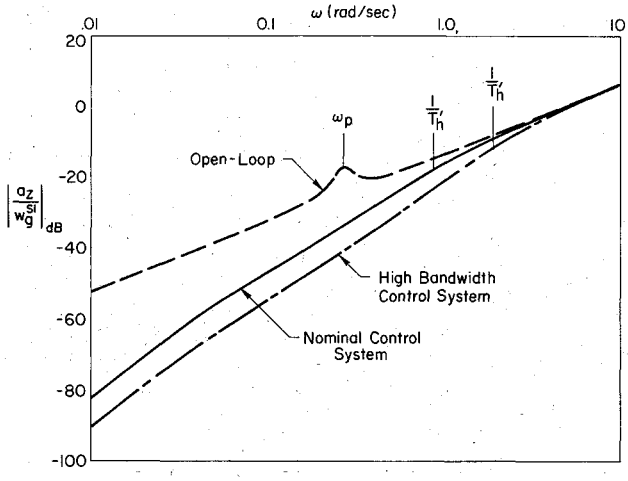

Fig. 5 Vertical acceleration response to gust inputs at source 1, a_z/w_g^{s1}.

freely away from the mooring mast in severe turbulence conditions.[9] Also, current Goodyear policy[13] is to allow the moored airship to freely "kite," thereby relieving the otherwise large air mass forces associated with constraining the vehicle against its natural convective motion.

The closed-loop response below the augmented heave mode ($1/T_h'$) is significantly reduced from the open-loop case, due to the desired function of the (nominal) vertical axis control system. The pitch axis control system damps the previous excitation of the open-loop pitch mode, ω_p. Additional increases in the vertical loop bandwidth are shown in Fig. 5 to further reduce the vertical acceleration gust response. This is expected from the improved command response characteristics shown in Fig. 3. Again, the high-frequency characteristics (about $1/T_h'$) are unchanged, since the unsteady (accelerated flow) aerodynamics of the rotors are neglected.

The retention of significant acceleration responses out to high frequencies suggests potential interaction between the accelerometer measurements and structural (high-frequency modes), possibly causing degradation of the control system effectiveness and resulting gust suppression performance. Careful attention will have to be paid to insure that the accelerometers are located at appropriate points relative to the mode shapes of the dominant structural modes for appropriately tailored control system/structure interaction.

Constraint Force Response

The frequency response of vertical constraint force between the hull and LPU-1 due to gust inputs at source 1, ($F_{c_{z1}}/w_g^{s1}$), is shown in Fig. 6 for the open- and closed-loop vehicle. high-frequency response of $F_{c_{z1}}$ to each of the other remaining gust input sources is nearly identical, again due to the symmetry of the input sources about the hull, the relatively small tail and the constant hull response to gust accelerations. However, the low-frequency characteristics of the remaining transfer functions are quite different, especially near the open-loop pitch mode, ω_p. This results from the coupling of the constraint force and pitch mode responses due to the rotor damping forces.

Figure 6 shows a *significant increase* in the constraint force loads from the use of closed-loop control to regulate hull motion against turbulence. For the closure selected in the present study, the mid-frequency load response increases by a factor of 6. Further increases in the vertical gain indicate an inverse relation between vertical acceleration response suppression (a_z/w_g) and constraint force response amplification ($F_{c_{z1}}/w_g$). The *limiting condition* of a vertically constrained vehicle is being approached with this high bandwidth case.

The increase in constraint loads associated with the higher bandwidth control systems is due to the attempt of the rotors to restrain the hull in the presence of large *gust acceleration* loads. Reductions in quasisteady (i.e., velocity-dependent cross flow) forces, which arise from the closed-loop (stabilized) hull motion, are overshadowed by this effect. DeLaurier[1,15] cites such reductions in structural loads on classic airships with increases in control gain, since the gust acceleration dependent terms were not included in his dynamic model.

An important conclusion of this analysis is the existence of a direct tradeoff between requirements for precision control and structural integrity. This will be especially important for the hover and near-hover precision control tasks which are essential to the heavy lift airship logging and payload positioning roles. Design and performance specifications for these vehicles need to include this tradeoff.

Statistical Response to Turbulence

The statistics of the vertical acceleration (a_z) and vertical constraint force ($F_{c_{z1}}$) response to statistical turbulence were evaluated for the open-loop (control system not engaged) and several closed-loop systems. These analyses were based on the linearized decoupled longitudinal transfer functions of the previous section for a flight condition having an airspeed (V_a) of 44 ft/s (30 mph), with a headwind of 30 ft/s (20 mph), resulting in a groundspeed (V_0) of 14 ft/s (10 mph). The statistical analysis was completed using the following simplified first-order approximation of the Dryden spectrum:[12]

$$\Phi_{w_g w_g} = \sigma^2_{w_g}\left(\frac{3V_a}{\pi L_{w_g}}\right)\left[\frac{1}{s+(3V_a/2L_{w_g})}\right]^2 \qquad (4)$$

The following numerical values were selected, based on the guidelines given in Ref. 10, for the given flight condition at an altitude of 2000 ft:

σ_{w_g} = 6.4 ft/s = intensity level for "moderate turbulence"
L_{w_g} = 1750 ft = turbulence scale length

As previously discussed, the assumed applicability of the four-point atmospheric input model is limited to turbulent wavelengths not exceeding two body lengths. In order to restrict the calculation of statistics to wavelengths within this limitation, a standard third-order Butterworth filter was used to truncate the input power spectral density function of Eq. (4). For the present flight condition, the Butterworth cutoff frequency is $\omega_c = \pi V_a/\ell_h = 0.57$ rad/s. Note that this cutoff frequency is a decade above the break frequency of the (simplified) Dryden input power spectral density filter; hence, the truncation of the spectrum will not represent a severe restriction of the analyses for this flight condition. The following truncated input power spectral density function is obtained by combining the simplified Dryden model with the Butterworth filter:

$$\Phi^*_{w_g w_g} = \Phi_{w_g w_g}\left[\frac{\omega_c^3}{(s+\omega_c)(s^2+\omega_c s+\omega_c^2)}\right] \qquad (5)$$

where the asterisk denotes that the input power spectrum has been truncated.

The output root mean square (rms) value for a response to a specific gust input source is obtained as

$$\sigma^2 = \int_0^\infty \Phi^*_{w_g w_g}\,|G(j\omega)|^2 \mathrm{d}\omega \qquad (6)$$

where $G(j\omega)$ are the complex transfer functions, typified by (a_z/w_g^{s1}) and $(F_{c_{z1}}/w_g^{s1})$, discussed earlier.

The total response to all four gust input sources is obtained by superposition, as explained earlier. For example, the total vertical acceleration rms response (σa_z) is calculated from:

$$\sigma a_z = [\sigma^2(a_z/w_g^{s1}) + \sigma^2(a_z/w_g^{s2}) + \sigma^2(a_z/w_g^{s3}) + \sigma^2(a_z/w_g^{s4})]^{1/2} \qquad (7)$$

A statistical analysis of vertical acceleration and constraint force response to turbulence was completed. The output rms levels were normalized by the turbulence intensity (σ_{w_g}) and converted to decibels (dB) to allow easy scaling to other intensity levels. These results are shown in Fig. 7 as a function of the heave control system bandwidth, ω_{BW_h}.

As expected from the previous transfer function results, the vertical acceleration rms response decreases with increasing closed-loop bandwidth. Associated with this acceleration response reduction is an increase in the constraint force response. As the gain (and associated bandwidth) of the heave control system is increased, the acceleration response asymptotically approaches zero as the constraint force response approaches a constant value. These asymptotic values are representative of a vertically constrained condition (i.e., infinite closed-loop bandwidth).

The assumption of a constrained condition would provide a simplified approach for specifying extreme random load design requirements, for example, for fatigue and failure mode analyses. Such assumptions have been previously used to determine structural loads on classical airships.[14] One possible design requirement might be the 2σ constraint-force level, which could be expected roughly 2% of the time in a given turbulence flight condition. For the present flight condition, the 47.7 dB ratio of $\sigma F_{c_{z1}}/\sigma_{w_g}$ shown in Fig. 7 indicates a 2σ requirement of 3100 lb (above trim). This criterion does not appear to be an overly conservative estimate of the nominal closed-loop level for statistical loads analyses. However, the results in the next section show that, for discrete

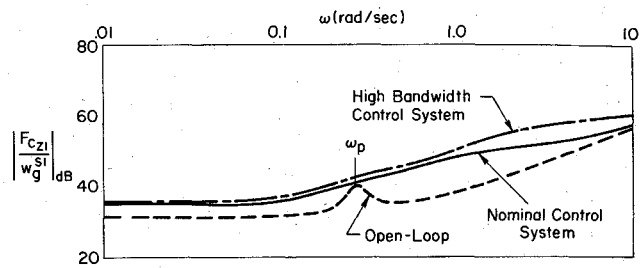

Fig. 6 LPU-1/Hull vertical constraint force response to gust inputs at source 1, $F_{c_{z1}}/w_g^{s1}$.

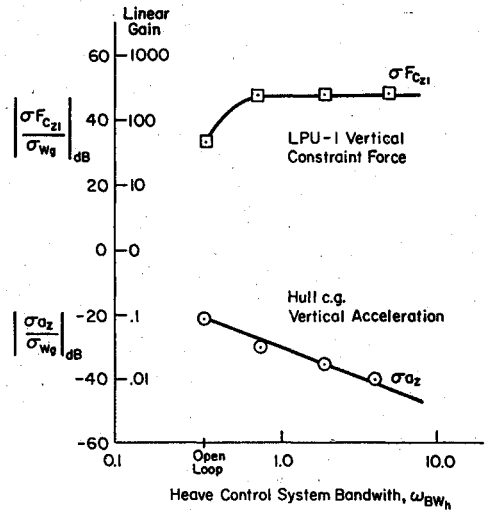

Fig. 7 Statistical response to turbulence.

turbulence encounters, a design requirement based on constrained motion would be very stringent, leading to an undesirably heavy structure.

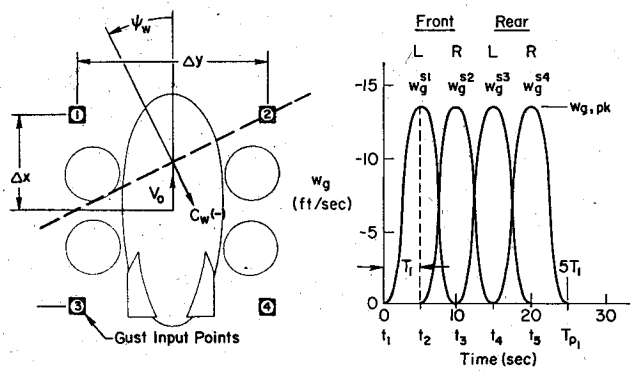

Parameter	Formulas
Dominant pitch mode period; T_p	$T_p = 2\pi/\omega_p$ (open-loop; $\omega_p \rightarrow \omega_p'$ for closed-loop)
Rise time ≡ peak spacing; T_I	$T_I = 0.4\,\pi/\omega_p$
Onset times; t_1, t_2, t_3, t_4	$t_1 = 0;\ t_2 = T_I;\ t_3 = 2T_I;\ t_4 = 3T_I$
Waveform ($i = 1, 2, 3, 4$)	$w_g^{si}(t) = \begin{cases} 0; t < t_i \text{ or } t > t_i + 2T_I \\ 0.5\, w_{g,pk}\{1 - \cos[\pi(t - t_i)/T_i]\} \\ \text{otherwise} \end{cases}$
Encounter angle from nose; ψ_w	$\psi_w = \tan^{-1}(\Delta x/\Delta y)$
Inertial crest celerity (crest velocity with respect to ground; positive means traveling same direction past hull as V_0)	$C_w = (V_0 - \Delta x/T_I)\cos\psi_w$

Fig. 8 Tuned oblique traveling upgust relationships.

The results of these statistical analyses re-emphasize the previous transfer function results concerning the tradeoff between requirements for response suppression and structural integrity. A significant increase in the constraint forces occurs with the implementation of any inertially referenced closed-loop control system. This suggests that the low-speed and precision-hover tasks, which require large flight control bandwidths, are critical for both disturbance suppression and structural load considerations. Further analyses are required to examine the moored flight condition, where large nose loads are expected to occur from the partially constrained condition.

Vehicle Nonlinear Response to a Tuned Discrete Gust Input

The discrete gust input is designed to excite the vehicle at its natural pitch and roll mode frequencies to provide information on critical motions and loads. This is conveniently done by having the vehicle encounter an obliquela oriented traveling upgust wave, whose celerity (inertially referenced crest velocity), wavelength, and relative heading are adjusted to maximally and simultaneously excite the pitch and roll modes. Here the wave is simulated by applying a tuned series of (1-cosωt) gusts at the four input sources and by properly selecting the wavelength and timing. The procedure is summarized in Fig. 8.

The present flight condition is an airspeed of 44 ft/s and a windspeed of 30 ft/s; the natural frequencies are 0.273 rad/s in pitch and 0.447 rad/s in roll. With the symmetrical 100-ft spacing of the gust input sources, the procedure yields an apparent wave encounter (ψ_w) angle of 27 deg from the nose (Fig. 2), a crest celerity (C_w) of 5.4 ft/s (Fig. 2), and (overlapping) input periods of 5 s for each source (Fig. 8). The selected peak gust magnitude of 13.4 ft/s results in the four gust inputs (one at each input source) which are shown in Fig. 8. This peak gust value is 44.7% of the mean windspeed of 30 ft/s. It was obtained from the military specification

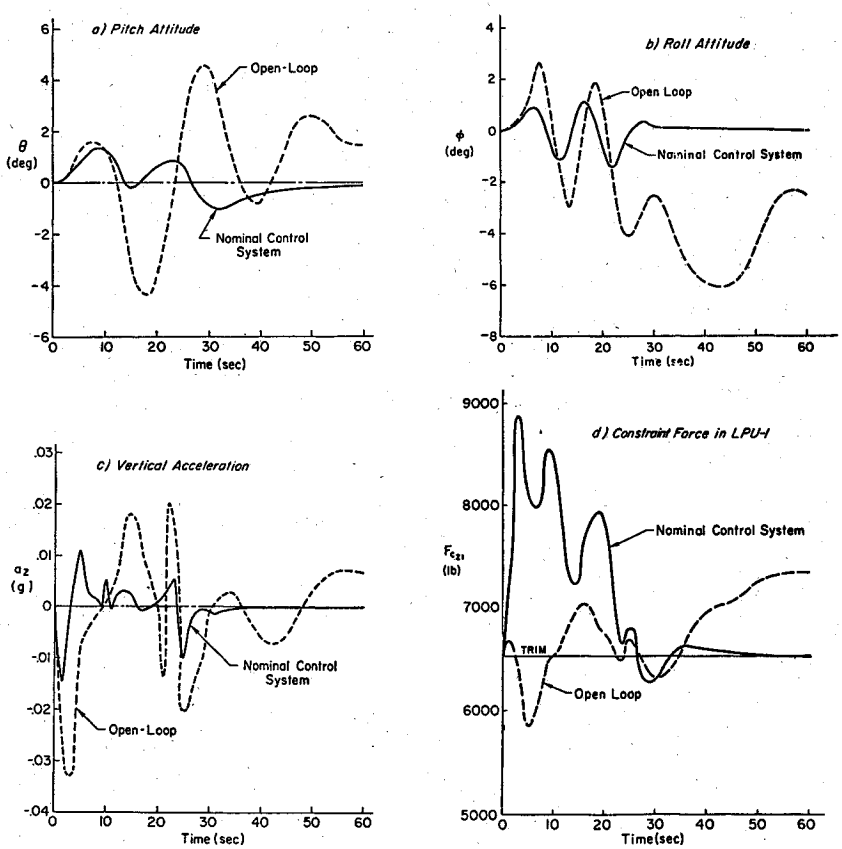

Fig. 9 Nonlinear open- and closed-loop responses to a tuned traveling oblique upgust.

requirements to be consistent with the previous statistical rms level for free-air turbulence.

Peak values expected in thunderstorm encounters by conventional aircraft are specified as a function of airspeed in the military specifications. An alternate peak value based on typical airship scenarios has been proposed.[3] The selection of an appropriate thunderstorm peak value and vehicle penetration airspeed is crucial to the resulting load requirements and depends largely on the specific mission and allowable operational weather conditions. For the present generic study, an analysis of extreme gust encounters has not been completed; however, the trends obtained using the moderate 13.4 ft/s gust are representative of the results that may be expected for more severe gust levels.

The open-loop pitch (θ) and roll (ϕ) responses (dashed lines in Figs. 9a and 9b) to the 13.4 ft/s peak upgust show that the vehicle is being excited at its damped natural frequencies. As expected from the linearized responses, the attitude and acceleration excursions (Figs. 9a-c) are significantly reduced due to the desired operation of the closed-loop flight control system. Strickly speaking, the oblique upgust parameters should be retuned to the closed-loop natural frequencies, but this was not done here.

In the open-loop case, the vertical constraint force in LPU-1 (Fig. 9d) responds at the same frequency (but roughly 180 deg out of phase) as the (open-loop) pitch response. A significant increase in the constraint force excursions and frequency results from the operation of the closed-loop system with the transient forces (from trim values) rising from about 600 to over 2300 lb. This is largely due to the attempt of the rotors to restrain the vehicle in the presence of large relative air-to-hull acceleration loads on the hull. The importance of these unsteady aerodynamic loads, compared with the quasisteady forces (those due to relative velocities), has been previously discussed and demonstrated.[8] The gradual rise in the open-loop constraint force, at the end of the time history, arises from the steady increase in relative vertical airspeed due to unstable vehicle lateral characteristics,[8] as reflected in Figs. 9a and 9b.

As discussed earlier herein, increasing the tightness (bandwidth) of the closed-loop system causes the constraint forces to approach the limiting values for an inertially restrained vehicle. Then the forces are just those that arise from the gust inputs. For the selected flight condition and discrete gust inputs, this limiting case yields a maximum constraint force load of 19,500 lb. The incremental load of 13,000 lb (above trim) is five times that (2300 lb) obtained for the nominal control system. While the constrained vehicle approximation provides a reasonable estimate for statistical turbulence analyses, this approximation is seen to be overly conservative for the analysis of discrete gust encounters, thereby leading to an overdesigned structure. Especially unrealistic loads are to be expected from similar analyses of thunderstorm-level discrete gust encounters where peak values exceed 35 ft/s.[3,10]

The constrained-vehicle calculation suggests that large loads would be imparted to a vehicle in a fully restrained mooring condition. The necessity of allowing unrestrained angular motion to relieve the otherwise large nose moments suggests the advantages of utilizing a mooring system that allows increased, but properly impeded, linear motion in order to relieve the associated nose forces.

The nonlinear time history responses underscore the results of the previous linearized analysis. The responses verify the earlier conclusion that a closed-loop reduction in acceleration response due to gust inputs is gained at the expense of significant transient increases in the constraint forces between the LPUs and the hull. Further increases in control system tightness accentuate this penalty. The increase in the constraint force frequency characteristics reflects higher-loop bandwidths and implies increased fatigue loads in the LPU and hull support structure. These fundamentally opposing trends require consideration in the flight control system performance and design load specification process.

A flight test program intended to verify the results presented herein would be very desirable. The key experimental requirement is accurate measurement of the gust disturbance input velocities at the four input locations about the airship and correction or "calibration" of such measurements in order to account for uncertain power and hull interference effects. Such measurement and calibration could conceivably be accomplished with power-off and -on tests and the application of potential flow corrections about a more conventional lighter-than air ship. Correlation of in-flight and meteorological tower(s) or tethered balloon(s) measurements are additional experimental possibilities for extracting such calibrated data.

Conclusions

An analysis of typical quadrotor heavy-lift airship motions and loads due to atmospheric disturbance was completed. The results presented in this paper lead to the following conclusions.

1) Vehicle motions due to gust responses were maximum at frequencies corresponding to those of the airship's natural motions.

2) Loads between the rotor units and hull are dominated by static (trim) loads and the unsteady aerodynamic hull forces due to its acceleration relative to the gusting air mass.

3) Implementation of a multiaxis closed-loop control system not only causes a significant reduction in the vehicle dynamic motion to statistical and discrete gust inputs, but also causes large increases in the transient constraint forces between the hull and LPUs.

4) The loads computed by assuming that the vehicle is fully constrained by the lift/propulsion unit arms are overly conservative for cruise calculations, but they suggest the advantages of a compliant mooring system which would allow some linear motion impeded in a proper manner.

5) An extension of the aircraft military specification discrete tuned (1-cosωt) gust input for loads requirements is suggested. It simulates the effects of an oblique traveling upgust wave, tuned to simultaneously excite both pitch and roll dominant modes, for which constraint forces are worst.

6) The existence of tradeoffs between tight vehicle response and resulting increases in vehicle constraint forces suggests that closer attention than usual needs to be paid to operations in the low-speed and hover-flight regimes where gust responses are most significant. Future studies should focus on:

a) Opening up of motion tolerances for precision hover and load handling, for example, by different load-handling techniques.

b) Flight control laws that allow some high-frequency vehicle attitude and linear motions while constraining the low-frequency linear motions.

c) Hull and tail gust load relief (e.g., via tail controls responsive to hull gust angles or loads).

Acknowledgment

The work reported in this paper was sponsored by the National Aeronautics and Space Administration under Contract NAS2-10330. The Project Monitor was P. D. Talbot.

References

[1]DeLaurier, J. D. and Hui, K. C. K., "Airship Survivability in Atmospheric Turbulence," *A Collection of Technical Papers; Proceedings of AIAA Lighter-Than-Air Systems Technology Conference,* Annapolis, M., July 1981, pp. 48-61.

[2]Nagabhushan, B. L. and Tomlinson, N. P., "Dynamics and Control of a Heavy Lift Airship in Cross Wind Hover," *A Collection*

of Technical Papers; Proceedings of AIAA Lighter-Than-Air Systems Technology Conference, Annapolis, M., July 1981, pp. 90-95.

[3]Troller, T. H., "Airships in Gusts: Apprehensions and Assurance," AIAA Paper 75-950, *Proceedings of AIAA Lighter-Than-Air Technology Conference,* July 1975.

[4]Bailey, D. B. and Rappaport,H. K., *Maritime Patrol Airship Study (MPAS),* NADC-80149-60, March 1980.

[5]Ardema, M. D., "Vehicle Concepts and Technology Requirements for Buoyant Heavy-Lift Systems," NASA TP 1921, Sept. 1981.

[6]Fries, G. H. and Schneider, J. J., "HLH and Beyond," SAE Paper 791086, presented at Aerospace Meeting, Los Angeles, Dec. 1979.

[7]Tischler, M. B., Ringland, R. F., Jex, H. R., et al., "Flight Dynamics Analysis and Simulation of Heavy-Lift Airships," Technical Manual NASA CR166471, Vol II, Dec. 1982.

[8]Tischler, M. B., Jex, H. R., and Ringland, R. F., "Simulation of Heavy Lift Airship Dynamics Over Large Ranges of Incidence and Speed," *A Collection of Technical Papers; AIAA Lighter-Than-Air Systems Technology Conference,* Annapolis, M., July 1981, pp. 96-115.

[9]Etkin, B., "The Turbulence Wind and Its Effect on Flight," UTIAS Review 44,Aug. 1980 (AIAA Wright Brothers Lecture, 1980; summarized in AIAA Paper 80-1836).

[10]Anon., "Flying Qualities of Piloted Airplanes," MIL-F-8785C, Nov. 1980.

[11]Holley, W. E., and Bryson, Jr., A. E., "Wind Modeling and Lateral Aircraft Control for Automatic Landing," Stanford University Rept. SUDAAR 489, Jan. 1975.

[12]Jewell, W. F., "Gust Response of the Super King Air 200 Aircraft," Systems Technology, Inc., Tech. Rept. No. 2139-2R, July 1980.

[13]Anon., "Preliminary Study of Ground Handling Characteristics of Buoyant Quad Rotor (BQR) Vehicles," NASA CR-166130, July 1980.

[14]Burgess, C. P., *Airship Design,* Ronald Press Co., New York, 1927.

[15]DeLaurier, J. D., Schenck, D. M., and Hui, C. K., "An Investigation of the Operational Reliability of Large Airships in Regularly-Scheduled Missions", Research Report 68, April 1980.